Information Processing Letters 113 (2013) 132–136

Contents lists available at SciVerse ScienceDirect

Information Processing Letters

www.elsevier.com/locate/ipl

The complexity of geodesic Voronoi diagrams on triangulated 2-manifold surfaces

Yong-Jin Liu [a,*], Kai Tang [b]

[a] Tsinghua National Lab for Information Science and Technology, Department of Computer Science and Technology, Tsinghua University, Beijing, PR China
[b] Department of Mechanical Engineering, The Hong Kong University of Science and Technology, Hong Kong, China

ARTICLE INFO

Article history:
Received 28 January 2012
Received in revised form 19 June 2012
Accepted 27 December 2012
Available online 2 January 2013
Communicated by R. Uehara

Keywords:
Voronoi diagram
Triangulated surfaces
Combinatorial complexity
Computational geometry

ABSTRACT

We study the combinatorial complexity of Voronoi diagram of point sites on a general triangulated 2-manifold surface, based on the geodesic metric. Given a triangulated 2-manifold T of n faces and a set of m point sites $S = \{s_1, s_2, \ldots, s_m\} \in T$, we prove that the complexity of Voronoi diagram $V_T(S)$ of S on T is $O(mn)$ if the genus of T is zero. For a genus-g manifold T in which the samples in S are dense enough and the resulting Voronoi diagram satisfies the closed ball property, we prove that the complexity of Voronoi diagram $V_T(S)$ is $O((m+g)n)$.

1. Introduction

On an orientable triangulated 2-manifold T, the Voronoi diagram of a set of point sites based on the geodesic metric [10] (called below *geodesic Voronoi diagram* for short) has found a wide range of applications in pattern analysis and computer vision [7]. More precisely, given a set of m distinct sample points $S = \{s_1, s_2, \ldots, s_m\}$ on T, the geodesic metric $d_g(\cdot)$ induces a Voronoi diagram $V_T(S)$ of S on T which subdivides T into m cells, one for each point in S:

$$V_T(S) = \{V(s_1), V(s_2), \ldots, V(s_m)\}$$

such that each cell satisfies

$$V(s_i) = \{p \in T \mid d_g(s_i, p) \leqslant d_g(s_j, p), \quad i \neq j,\ j \in \{1, 2, \ldots, m\}\}$$

1.1. Geodesic metric d_g on T

A saddle vertex in T is defined as a vertex for which the sum of incident angles of surrounding triangles is greater than or equals 2π. A geodesic path between any two points p, q on T is a locally shortest path l connecting p and q on T. The path l goes through a series of triangles which can be unfolded into a common 2D plane ϖ as shown in Fig. 1. In ϖ, path l becomes either a line segment $\overline{pq}$ or a polyline $\overline{pv_1v_2\cdots v_kq}$, for which Mitchell et al. [8] showed that $v_1, v_2, \ldots, v_k$ can only be saddle vertices in T. The geodesic distance $d_g(p, q)$ is the length of the shortest geodesic path between p, q on T.

1.2. Structural properties of $V_T(S)$ on T

Points in S are called *sites* of Voronoi diagram $V_T(S)$. A *Voronoi edge* is the intersection of two Voronoi cells and a *Voronoi vertex* is the intersection of three or more Voronoi cells. Upon a sufficiently small perturbance [4], we use the following assumptions:

* Corresponding author.
E-mail addresses: liuyongjin@tsinghua.edu.cn (Y.-J. Liu), mektang@ust.hk (K. Tang).

0020-0190/$ – see front matter
http://dx.doi.org/10.1016/j.ipl.2012.12.010

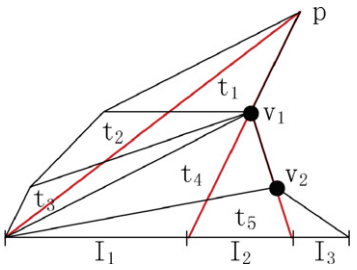

Fig. 1. Geodesic paths inside triangles $(t_1, t_2, t_3, t_4, t_5)$ folded into a plane. For the source point p, if the inquiry point $q \in I_1$, then the shortest path is a line $\overline{pq}$; if $q \in I_2$ (or $q \in I_3$), the shortest path is a polyline $\overline{pv_1q}$ (or $\overline{pv_1v_2q}$).

Assumption 1. No vertices in T have the same geodesic distance to any two sites in S.

Assumption 2. Any saddle vertex in T has a unique geodesic path to each site in S.

Given Assumption 1, we have:

- Each Voronoi edge is 1D, i.e., homeomorphic to either a line segment or a circle.
- All Voronoi cells are bounded by Voronoi edges, mutually exclusive or semi-exclusive, and $\bigcup_{i=1}^{m} V(s_i) = T$.

For a triangulated 2-manifold T of arbitrary genus, any Voronoi cell $V(s_i)$ is path-connected, possibly bounded by several closed Voronoi edges. Different from planar Voronoi diagram, a Voronoi edge in $V_T(S)$ may be closed itself, i.e., without ending at a Voronoi vertex. Fig. 2 shows such an example. Any Voronoi edge is a trimmed bisector of two sites in S on T. We assign a *binary relation* (s_i, v_i) to each point p inside a Voronoi cell $V(s_i)$, where v_i is the closest saddle vertex to p in the geodesic path connecting s_i and p, or $v_i = s_i$ if there is no saddle vertex in the path. For each point in the Voronoi edge, it corresponds to two binary relations (s_i, v_i) and (s_j, v_j), and we use $B_{s_is_j}(v_i, v_j)$ to denote the portion in a Voronoi edge contributed by $(s_i, v_i), (s_j, v_j)$.

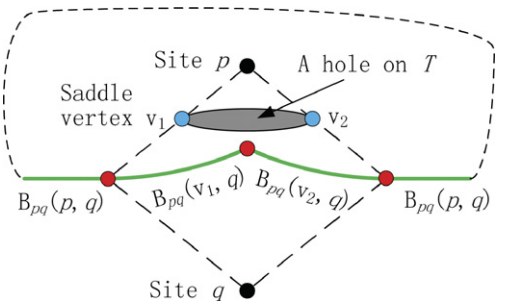

Fig. 3. Breakpoints (shown in red) in a Voronoi edge B_{pq} shared by two Voronoi cells $V(p)$ and $V(q)$. B_{pq} consists of three portions, $B_{pq}(p, q)$, $B_{pq}(v_1, q)$, $B_{pq}(v_2, q)$. The shaded hole can be a polygonal obstacle such as a prism of sufficient height. (For interpretation of the references to color in this figure legend, the reader is referred to the web version of this article.)

Definition 1. A breakpoint in a Voronoi edge $B_{s_is_j}$ contributed by sites s_i, s_j, is a transition point at which the portion of the Voronoi edge changed from $B_{s_is_j}(v_i, v_j)$ to $B_{s_is_j}(v_k, v_l)$, where the unordered pairs $(v_i, v_j) \neq (v_k, v_l)$.

Fig. 3 shows an illustration of breakpoint definition. We define the *combinatorial complexity* of $V_T(S)$ to be the total number of breakpoints, Voronoi vertices, Voronoi edges and Voronoi cells in $V_T(S)$.

1.3. Related work

Moet et al. [9] studied a special triangulated surface, called *realistic terrain*, which is a piecewise-linear continuous function defined over a planar triangulation. Moet et al. showed that the Voronoi diagram of m sites on an n-face realistic terrain has complexity $\Omega(n + m\sqrt{n})$ and $O((n+m)\sqrt{n})$. Aronov et al. [1] improved the results in [9] and showed that the worse-case complexity of the Voronoi diagram on a realistic terrain is $\Theta(n+m\sqrt{n})$. Cabello et al. [2] studied the higher-order Voronoi diagrams on triangulated surfaces and showed that the sum of the combinatorial complexities of the order-j Voronoi diagrams of m sites on an n-face triangulated surface, for $j = 1, 2, \ldots, k$, is $O(k^2n^2 + k^2m + knm)$. Note that the work in [2] used

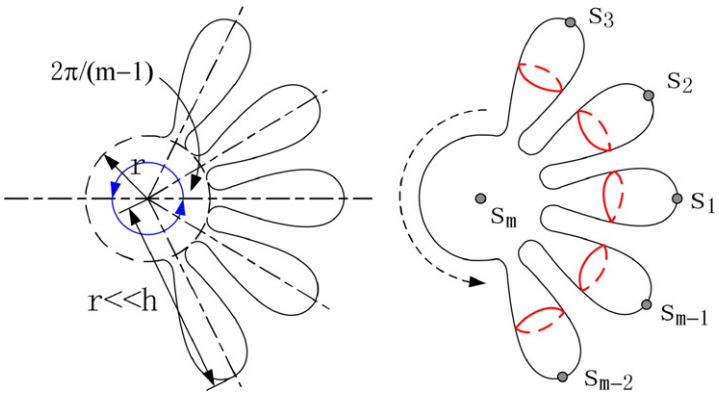

Fig. 2. The Voronoi diagram of sites in S (shown in grey points) on a 2-manifold model. All the Voronoi edges (shown in red) are homeomorphic to a circle and there is no Voronoi vertex in this diagram. The Voronoi cell $V(s_m)$ has $m-1$ closed Voronoi edges. (For interpretation of the references to color in this figure legend, the reader is referred to the web version of this article.)

a different meaning of combinatorial complexity, by including the number of edges on T that are crossed by Voronoi edges as breakpoints. Our definition of breakpoints is consistent with the ones in [1,9].

1.4. Our results

We study the combinatorial complexity of Voronoi diagram $V_T(S)$ on a general triangulated surface T. Previous work [1,9] on a special terrain model gave the lower bound $\Omega(n+m\sqrt{n})$. But for a general surface T of arbitrary genus, no upper bound is provided. We present a simple yet effective proof, showing that the complexity of Voronoi diagram of m sites on a general n-face T is $O(mn)$ if the genus of T is zero. For T of genus-g ($g > 0$) in which the samples in S are dense enough, we show that the complexity of Voronoi diagram $V_T(S)$ is bounded by $O((m+g)n)$.

2. Complexity of breakpoints in a Voronoi edge

In $V_T(S)$, $B_{s_i s_j}$ is denoted as the Voronoi edge contributed by sites s_i, s_j. At each breakpoint bk_i on $B_{s_i s_j}$, the shortest path from bk_i to s_i (or s_j) is not unique. Without loss of generality, let bk_i have two shortest paths $P_{s_i}(v_r), P_{s_i}(v_s)$ to s_i, $v_r \neq v_s$, where paths $P_{s_i}(v_r), P_{s_i}(v_s)$ go through respectively saddle vertices v_r, v_s in the binary relations assigned to bk_i. Given that paths $P_{s_i}(v_r), P_{s_i}(v_s)$ cannot intersect each other (based on Assumption 2) and they are both completely contained in the Voronoi cell $V(s_i)$, we denote the connected region in $V(s_i)$ by $Area(P_{s_i}(v_r), P_{s_i}(v_s))$ whose boundaries are formed by $P_{s_i}(v_r) \cup P_{s_i}(v_s)$.

Property 1. *$Area(P_{s_i}(v_m), P_{s_i}(v_n)) \in V(s_i)$ can enclose one or more Voronoi cells $V(s_{k_r})$, $r = 1, 2, \ldots, l$, $l < m$, $s_{k_r} \neq s_i$, $s_{k_r} \neq s_j$.*

We demonstrate this property by constructing an example. We put a cone of sufficient hight at the shaded hole in the configuration shown in Fig. 3 and redraw it in Fig. 4. Let bk_r be a breakpoint in the edge $B_{s_i s_j}$. In $V(s_i)$, there are two shortest paths $P_{s_i}(v_1), P_{s_i}(v_2)$ from bk_r to s_i. Let site s_k sit on the apex of the cone. Since the height of the cone is sufficient large, $Area(P_{s_i}(v_1), P_{s_i}(v_2)) \in V(s_i)$ completely encloses the Voronoi cell $V(s_k)$. Similarly if we put more cones inside $Area(P_{s_i}(v_1), P_{s_i}(v_2))$ akin to the fingers in a hand and put a site on the apex of each cone, the Voronoi cells of these sites will be all enclosed by $Area(P_{s_i}(v_1), P_{s_i}(v_2))$. In this case, the shortest paths $P_{s_i}(v_1), P_{s_i}(v_2)$ are not homologous in $V(s_i)$.

One Voronoi cell $V(s_i)$ may be multiple-connected and let $L(s_i)$ be one of its closed boundaries. Denote all breakpoints in $L(s_i)$ as $BK_{L(s_i)} = \{bk_1, bk_2, \ldots, bk_s\}$ and $SV_{L(s_i)} = \{sv_1, sv_2, \ldots, sv_t\}$ as the union of all saddle vertices in $V(s_i)$ that constitute binary relations with $BK_{L(s_i)}$. Breakpoints in $BK_{L(s_i)}$ are ordered such that when one walks from $bk_{(j \bmod s)}$ to $bk_{(j+1 \bmod s)}$, the interior of $V(s_i)$ always lies to the left hand side. Whenever there is no risk of confusion, we omit the operator mod s below.

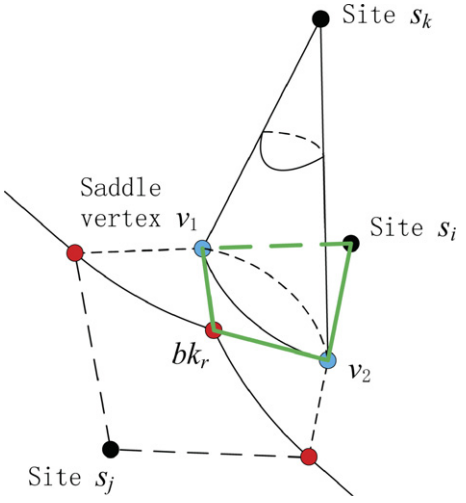

Fig. 4. $Area(P_{s_i}(v_1), P_{s_i}(v_2))$ in the Voronoi cell $V(s_i)$ encloses another Voronoi cell $V(s_k)$, where the path $P_{s_i}(v_1)$ starts from s_i to breakpoint bk_r through v_1, and $P_{s_i}(v_2)$ through v_2, and site s_k sits on an apex of a cone of sufficient height.

Lemma 1. *Each saddle vertex in $SV_{L(s_i)}$ can devote to at most two breakpoints in $BK_{L(s_i)}$. Here "an sv devotes to a bk" means there is a shortest path from bk to a site through sv.*

Proof. breakpoints in $BK_{L(s_i)}$ separate $L(s_i)$ into pieces. For any point inside each piece, there is only one shortest path to s_i going through a saddle vertex $sv \in SV_{L(s_i)}$. Since sv enters and leaves the binary relations for points in one piece at two endpoints, sv devotes to these two breakpoints. Assume sv devotes to three breakpoints in $BK_{L(s_i)}$. Then two cases exist. First, the three breakpoints bk_i, bk_{i+1}, bk_{i+2} devoted by sv are consecutive along the Voronoi edge (Fig. 5 left). In this case, points in the piece $pe_1 = (bk_i, bk_{i+1})$ and points in the piece $pe_1 = (bk_{i+1}, bk_{i+2})$ have the same binary relation indicating the shortest path to s_i, and then bk_{i+1} cannot be a breakpoint. In the second case, sv devotes to bk_i, bk_{i+1}, bk_w, $w > i+2$ or $w < i-1$. In this case, however, either the shortest path from bk_{i+2} to s_i or the shortest path from bk_{i-1} to s_i must intersect the path $P_{s_i}(sv)$ started at bk_w (Fig. 5 right), a contradiction to the fact that given Assumption 2, two shortest paths to s_i cannot intersect each other. □

Denote the number of saddle vertices in $V(s_i)$ as $sn(s_i)$. Since any Voronoi edge e is incident to two Voronoi cells of s_i and s_j, the number of breakpoints in e is at most $2(sn(s_i) + sn(s_j))$.

3. Complexity of $V_T(S)$ on T of genus-0

Lemma 2. *The number of the Voronoi vertices and Voronoi edges in $V_T(S)$ on a genus-0 T is $O(m)$, where $m = \#S$ is the cardinality of S.*

Proof. Denote $\#\Phi$ as the cardinality of set Φ. Let $G(Ver(V_T(S)), Eg(V_T(S)))$ be the graph made up of all Voronoi vertices $Ver(V_T(S))$ and all Voronoi edges $Eg(V_T(S))$ in $V_T(S)$. By Property 1, there may be some

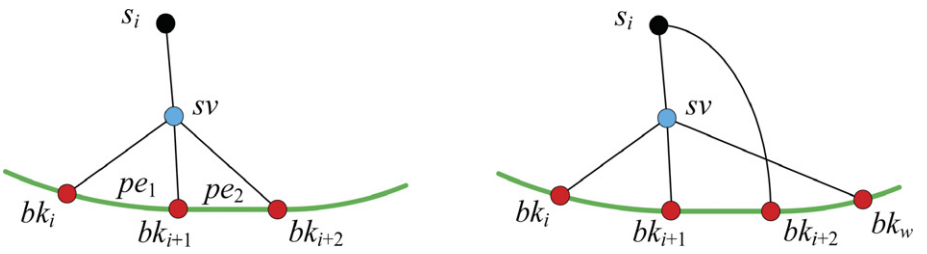

Fig. 5. Proof of Lemma 1.

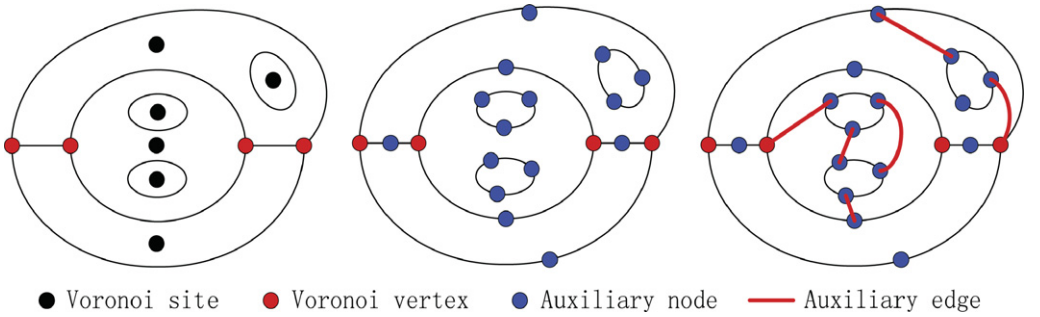

Fig. 6. Proof of Lemma 2. Left: the Voronoi diagram $V_T(S)$. Middle: the simple graph $\mathcal{G}'$ by adding auxiliary nodes. Right: the 2-connected graph $\mathcal{G}''$ by adding auxiliary edges.

Voronoi cells $V(s_i)$ that are completely surrounded by another Voronoi cell $V(s_j)$, $i \neq j$. Refer to Fig. 6 left. Let $Eg(V_T(S)) = E_{loop} \cup E_{piece}$, where E_{loop} is the subset of Voronoi edges, each of which is homeomorphic to a circle and E_{piece} is the subset of Voronoi edges, each of which is homeomorphic to a line segment. We introduce three auxiliary nodes into each edge in E_{loop} and one auxiliary node into each edge in E_{piece}, as shown in Fig. 6 middle. Denote the resulting graph by $G' = (V', E')$, where $\#V' = \#Ver + \#E_{piece} + 3\#E_{loop}$ and $\#E' = 2\#E_{piece} + 3\#E_{loop}$. G' is a simple graph but may not be 2-connected. We add edges between vertices from different components in G', leading to a 2-connected graph G'' as shown in Fig. 6 right. Denote the edges in $G'' \setminus G'$ by E_{add}. By Fary's theorem, G'' on a genus-0 T has a planar embedding and thus Euler's formula holds. Note that there are m faces in G' and each new added edge in E_{add} can split one Voronoi cell into at most two. We have

$$\#E'' - \#V'' + 2 \leqslant m + \#E_{add}$$

Since

$$\#E'' = \#E' + \#E_{add}, \qquad \#V'' = \#V'$$

$$\#V' = \#Ver + \#E_{piece} + 3\#E_{loop}$$

$$\#E' = 2\#E_{piece} + 3\#E_{loop}$$

we have

$$\#E_{piece} - \#Ver + 2 \leqslant m$$

Since $2\#E_{piece} \geqslant 3\#Ver$ and $\#E_{loop} \leqslant m$, we have $\#Ver = O(m)$ and $\#Eg = O(m)$. □

Theorem 1. *The combinatorial complexity of $V_T(S)$ on T of genus-0 is $O(mn)$, where n is the number of faces in T.*

Proof. By Lemma 1, each Voronoi edge can have at most $O(n)$ breakpoints. Given Lemma 2, there are totally $O(mn)$ breakpoints and $O(m+n)$ Voronoi vertices, edges and cells. □

4. Complexity of $V_T(S)$ on T of genus-g

$V_T(S)$ is called an *intrinsic Voronoi diagram* which satisfies the closed ball property [5] if and only if:

- Each Voronoi cell is a closed topological disk.
- The intersection of two Voronoi cells is either empty or a single Voronoi edge.
- The intersection of three Voronoi cells is either empty or a single Voronoi vertex.

It was shown in [3,6] that given a sampling S of T, if $\forall x \in T$, $\exists s_i \in S$, such that $s_i \in B(x, \rho_m(x))$, then $V_T(S)$ satisfies the closed ball property, where $B(x,r) = \{y \in T : d_g(x,y) < r\}$, $\rho_m(x) = \min\{conv(x), \frac{1}{2} inj(x)\}$, $conv(x)$ and $inj(x)$ are convexity radius and injectivity radius of x, respectively [3].

Lemma 3. *The number of the Voronoi vertices and edges in an intrinsic Voronoi diagram $V_T(S)$ on the genus-g T is $O(m+g)$, where $m = \#S$.*

Proof. Since $V_T(S)$ satisfies the closed ball property, it is proved in [3] that the dual of $V_T(S)$ exists and is a proper triangulation of the underlying 2-manifold. So the Euler's formula $\#Edge - \#Vertex + 2 - 2g = \#Face$ is applicable to $V_T(S)$. □

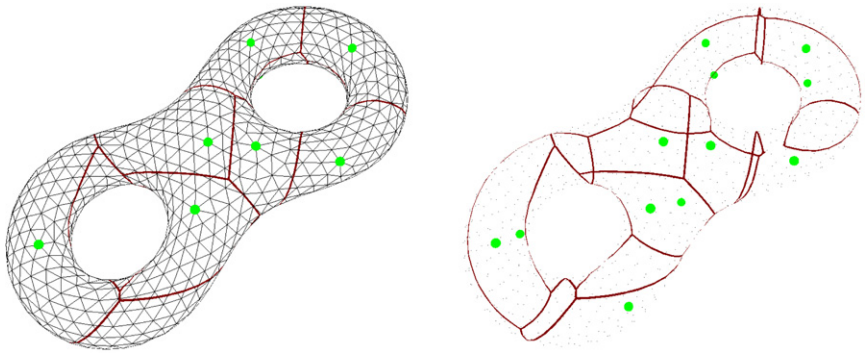

Fig. 7. The Voronoi diagram of 12 sites on a 2022-face triangulated surface of genus-2. Left: the Voronoi diagram on the triangulated surface. Right: the Voronoi edges and sites with transparent surface.

Theorem 2. *If the sampling S on T is dense enough such that $V_T(S)$ satisfies the closed ball property, the combinatorial complexity of $V_T(S)$ on T of genus-g is $O((m+g)n)$.*

5. Conclusions

We study the combinatorial complexity of Voronoi diagram $V_T(S)$ on a general triangulated 2-manifold T of arbitrary genus g. The bound $O((m+g)n)$ offers a theoretical guarantee of polynomial complexity in space and time for the practical algorithm in [7]. A real world example is shown in Fig. 7. In particular, we show that the number of Voronoi vertices and Voronoi edges are linear with respect to the number of Voronoi cells in a 2-manifold of genus-0, serving as a direct generalization of the linear relationship in planar Voronoi diagrams.

Acknowledgements

This work is supported by the National Basic Research Program of China (2011CB302202), the 863 program of China (2012AA011801) and the Natural Science Foundation of China (61272228). The first author was also partially supported by Program for New Century Excellent Talents in University and TNList Cross-discipline Foundation.

References

[1] B. Aronov, M. de Berg, S. Thite, The complexity of bisectors and Voronoi diagrams on realistic terrains, in: 16th Annual Symposium on Algorithms (ESA 2008), 2008, pp. 100–111.
[2] S. Cabello, M. Fort, J.A. Sellares, Higher-order Voronoi diagrams on triangulated surfaces, Information Processing Letters 109 (9) (2009) 440–445.
[3] R. Dyer, H. Zhang, T. Moller, Surface sampling and the intrinsic Voronoi diagram, in: Proc. 24th Annu. ACM Sympos. Comput. Geom., 2008, pp. 1393–1402.
[4] H. Edelsbrunner, E.P. Mucke, Simulation of simplicity: a technique to cope with degenerate cases in geometric algorithms, ACM Transactions on Graphics 9 (1) (1990) 66–104.
[5] H. Edelsbrunner, N.R. Shah, Triangulating topological spaces, in: Proc. 10th Annu. ACM Sympos. Comput. Geom., 1994, pp. 285–292.
[6] W.Y. Gong, Y.J. Liu, K. Tang, T.R. Wu, 2-manifold surface sampling and quality estimation of reconstructed meshes, in: 2011 Eighth International Symposium on Voronoi Diagrams in Science and Engineering, 2011, pp. 15–22.
[7] Y.J. Liu, Z.Q. Chen, K. Tang, Construction of iso-contours, bisectors and Voronoi diagrams on triangulated surfaces, IEEE Transactions on Pattern Analysis and Machine Intelligence 33 (8) (2011) 1502–1517.
[8] J. Mitchell, D. Mount, C. Papadimitriou, The discrete geodesic problem, SIAM Journal on Computing 16 (4) (1987) 647–668.
[9] E. Moet, M. van Kreveld, A.F. van der Stappen, On realistic terrains, in: Proc. 22nd Annu. ACM Sympos. Comput. Geom., 2006, pp. 177–186.
[10] Y.J. Liu, Exact geodesic metric in 2-manifold triangle meshes using edge-based data structures, Computer-Aided Design 45 (3) (2013) 695–704.